Electronic Supplementary Material (ESI) for RSC Advances.
This journal is © The Royal Society of Chemistry 2015

Supporting Information

High HOMO Levels and Narrow Energy Band Gaps of Dithienogalloles

Takuya Matsumoto[a], Kazuo Tanaka*[a], and Yoshiki Chujo*[a]

[a] Department of Polymer Chemistry, Graduate School of Engineering, Kyoto University, Katsura, Nishikyo-ku, Kyoto 615-8510, Japan

General ^{1}H (400 MHz), and ^{13}C (100 MHz) NMR spectra were recorded on JEOL JNM-EX400 and JNM-AL400 spectrometers. ^{1}H and ^{13}C NMR spectra used tetramethylsilane (TMS) as an internal standard in $CDCl_3$, and C_6D_6. High-resolution mass spectra (HRMS) were obtained on a Thermo Fisher Scientific EXACTIVE for atomic pressure chemical ionization (APCI) and electron spray ionization (ESI). UV–vis spectra were recorded on a Shimadzu UV-3600 spectrophotometer. Fluorescence emission spectra were recorded on a HORIBA JOBIN YVON Fluoromax-4 spectrofluorometer, and the absolute quantum yield was calculated by integrating sphere method on the HORIBA JOBIN YVON Fluoromax-4 spectrofluorometer. Photoluminescence lifetime measurement was performed on a Horiba FluoreCube spectrofluorometer system; excitation was carried out using a UV diode laser (NanoLED 290 nm or 375 nm). X-ray crystallographic analysis was carried out by a Rigaku R-AXIS RAPID-F graphite-monochromated Mo Kα radiation diffractometer with an imaging plate. A symmetry related absorption correction was carried out by using the program ABSCOR[1]. The analysis was carried out with direct methods (SHELX-97[2] or SIR97[3]) using Yadokari-XG[4]. All reactions were performed under argon atmosphere.

Materials. All reagents were obtained from commercial sources and used without further purification. Tetrahydrofuran (THF) and diethyl ether (Et_2O) were purified using a two-column solid-state purification system (Glass Contour Solvent System, Joerg Meyer, Irvine, CA). Dichloro[2,6-di-*t*-butyl-4-(*N*,*N*-dimethylaminomethyl)phenyl]gallane (**MamxGaCl$_2$**)[5] and 4,4-dimethylcyclopenta[2,1-*b*:3,4-*b′*]dithiophene (**CDT**)[6] were prepared according to the literatures.

Computational Details. The Gaussian 09 program package[7] was used for computation. We optimized the structures of dithienoheteroles in the ground S_0 state and calculated their electronic structures. The density functional theory (DFT) was applied for the optimization of the structures in the S_0 state at the B3LYP/6-31G(d,p) levels. We calculated the electronic states and transitions from S_0 to S_1 states of the dithienoheteroles with the optimized geometries in the S_0 state by time-dependent DFT (TD-DFT) at the B3LYP/6-311+G(2df) levels for gallium atoms and the B3LYP/6-31G(d,p) levels for others.

Synthesis of GaDT. To a cold (−78 °C) solution of 3,3'-dibromo-2,2'-bithiophene (0.97 g, 3.0 mmol) in Et_2O (20 mL), *n*-BuLi (1.6 M in hexane, 4.2 mL, 6.6 mmol) was added dropwise. After the reaction mixture was stirred for 1.5 h, the mixture of **MamxGaCl$_2$**

(1.2 g, 3.2 mmol) and Et_2O (10 mL) was added to the solution at −78 °C. After warmed up to room temperature, the mixture was stirred for 1 day. The solution was diluted in chloroform, washed with brine and dried over Na_2SO_4. Recrystallization from methanol/chloroform gave a white solid (310 mg) in 21% yield. ^{1}H NMR (C_6D_6, δ, ppm): 7.61 (s, 1H), 7.07−7.04 (m, 4H), 6.95 (s, 1H), 3.26 (s, 2H), 1.77 (s, 6H), 1.38 (m, 18H); ^{13}C NMR (C_6D_6, δ, ppm): 159.5, 151.2, 150.5, 147.7, 143.5, 138.2, 132.21, 124.2, 121.8, 119.3, 67.2, 46.0, 36.9, 34.9, 32.2, 31.7. FTMS (APCI) m/z calcd $[M+H]^+$: 480.1305; found: 480.1303.

Synthesis of GaDT-TMS. To a cold (−78 °C) solution of 3,3'-dibromo-5,5'-trimethylsilyl-2,2'-bithiophene (1.8 g, 3.9 mmol) in Et_2O (30 mL), *n*-BuLi (1.6 M in hexane, 5.1 mL, 8.1 mmol) was added dropwise. After the reaction mixture was stirred for 1.5 h, the mixture of **MamxGaCl$_2$** (1.8 g, 4.6 mmol) and Et_2O (10 mL) was added to the solution at −78 °C. After warmed up to room temperature, the mixture was stirred for 1 day. The solution was diluted in chloroform, washed with brine and dried over Na_2SO_4. Recrystallization from methanol/chloroform gave a white solid (630 mg) in 26% yield. ^{1}H NMR ($CDCl_3$, δ, ppm): 7.47 (d, J = 1.6 Hz, 1H), 7.04−7.02 (m, 3H), 3.93 (s, 2H), 2.41 (s, 6H), 1.36 (s, 9H), 1.28 (s, 9H), 0.29 (s, 18H); ^{13}C NMR (C_6D_6, δ, ppm): 159.8, 156.7, 151.4, 150.7, 143.8, 140.0, 139.9, 138.7, 122.2, 119.6, 67.5, 46.2, 37.2, 35.1, 32.4, 31.9, 0.7. FTMS (APCI) m/z calcd $[M+H]^+$: 624.2095; found: 624.2082.

Synthesis of SiDT. To a cold (−78 °C) solution of 3,3'-dibromo-2,2'-bithiophene (1.3 g, 3.9 mmol) in THF (10 mL), *n*-BuLi (1.6 M in hexane, 5.1 mL, 8.3 mmol) was added dropwise. After the reaction mixture was stirred for 1 h, dichlorodimethylsilane (0.56 g, 520 μL, 4.3 mmol) was added to the solution at −78 °C. After warmed up to room temperature, the mixture was stirred for 8 h. The solution was diluted in chloroform, washed with brine and dried over $MgSO_4$. After the solvent was removed, the crude was purified by silica gel column chromatography using hexane. Recrystallization from methanol/chloroform gave a white solid in 17% yield. ^{1}H NMR ($CDCl_3$, δ, ppm): 7.20 (d, J = 4.9 Hz, 2H), 7.07 (d, J = 4.9 Hz, 2H), 0.41 (s, 6H); ^{13}C NMR ($CDCl_3$, δ, ppm): 149.0, 142.6, 129.2, 125.2, −3.5. FTMS (APCI) m/z calcd $[M+H]^+$: 223.0066; found: 223.0063.

Synthesis of SiDT-TMS. To a cold (−78 °C) solution of 3,3'-dibromo-5,5'-trimethylsilyl-2,2'-bithiophene (1.0 g, 2.1 mmol) in THF (10 mL), *n*-BuLi (1.6 M in hexane, 2.8 mL, 4.5 mmol) was added dropwise. After the reaction mixture was stirred for 1 h, dichlorodimethylsilane (0.30 g, 280 μL, 2.4 mmol) was added to the solution at −78 °C.

After warmed up to room temperature, the mixture was stirred for 8 h. The solution was diluted in chloroform, washed with brine and dried over $MgSO_4$. After the solvent was removed, the crude was purified by silica gel column chromatography using hexane. Recrystallization from methanol/chloroform gave a white solid (640 mg) in 70% yield. ^{1}H NMR ($CDCl_3$, δ, ppm): 7.17 (s, 2H), 0.41 (s, 6H), 0.33 (s, 18H); ^{13}C NMR ($CDCl_3$, δ, ppm): 154.4, 144.6, 141.3, 136.2, 0.1, −3.2. FTMS (APCI) m/z calcd $[M+H]^+$: 367.0856; found: 367.0853.

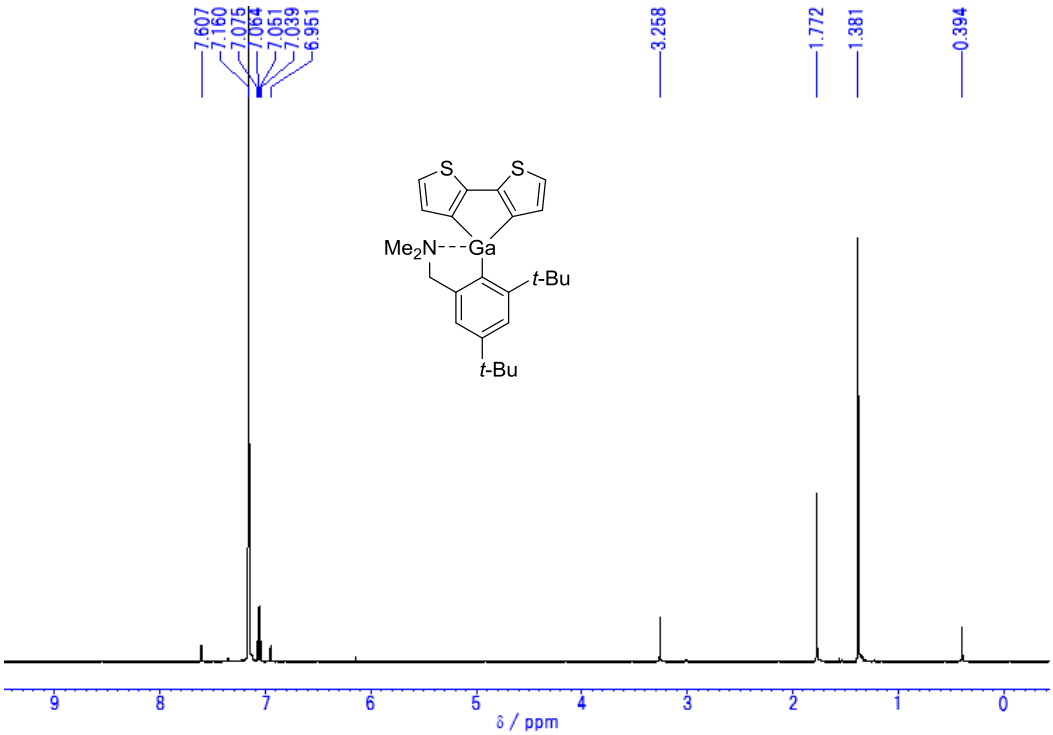

Figure S1. ^{1}H NMR spectrum of **GaDT** in C_6D_6.

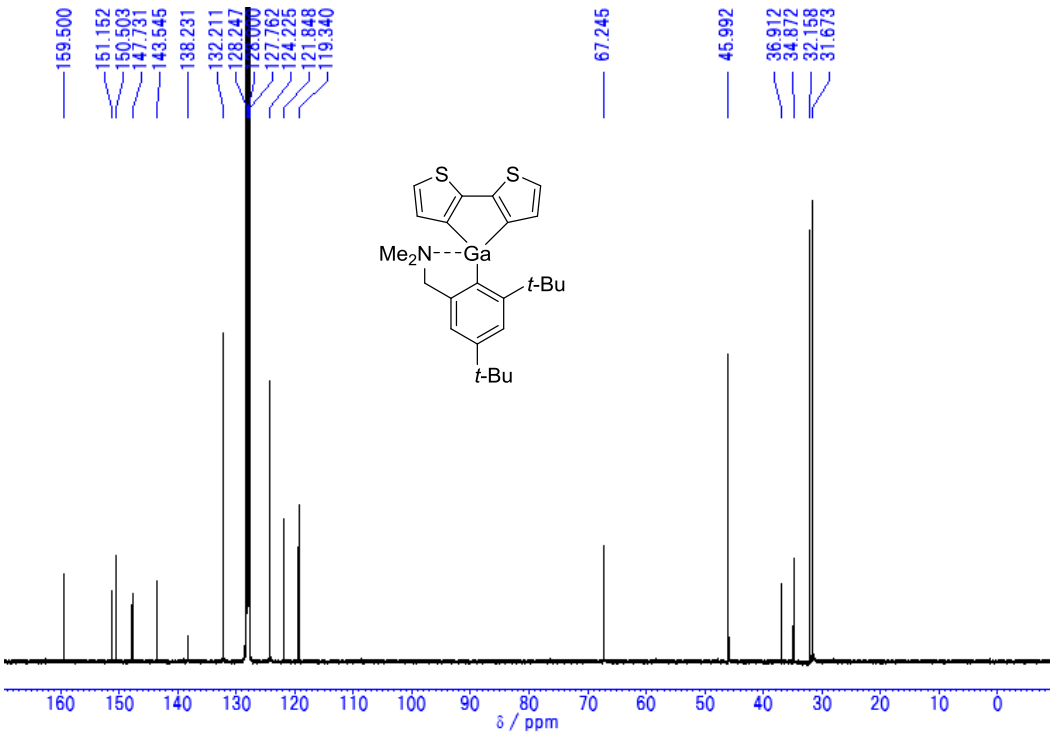

Figure S2. ^{13}C NMR spectrum of **GaDT** in C_6D_6.

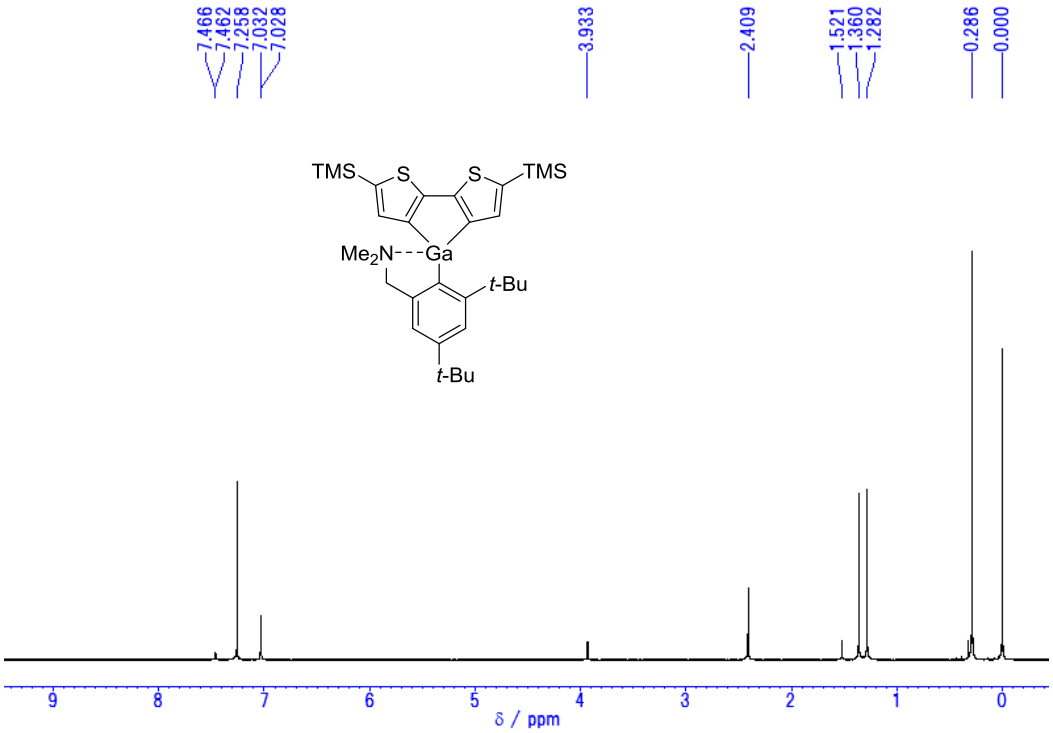

Figure S3. ^{1}H NMR spectrum of **GaDT-TMS** in $CDCl_3$.

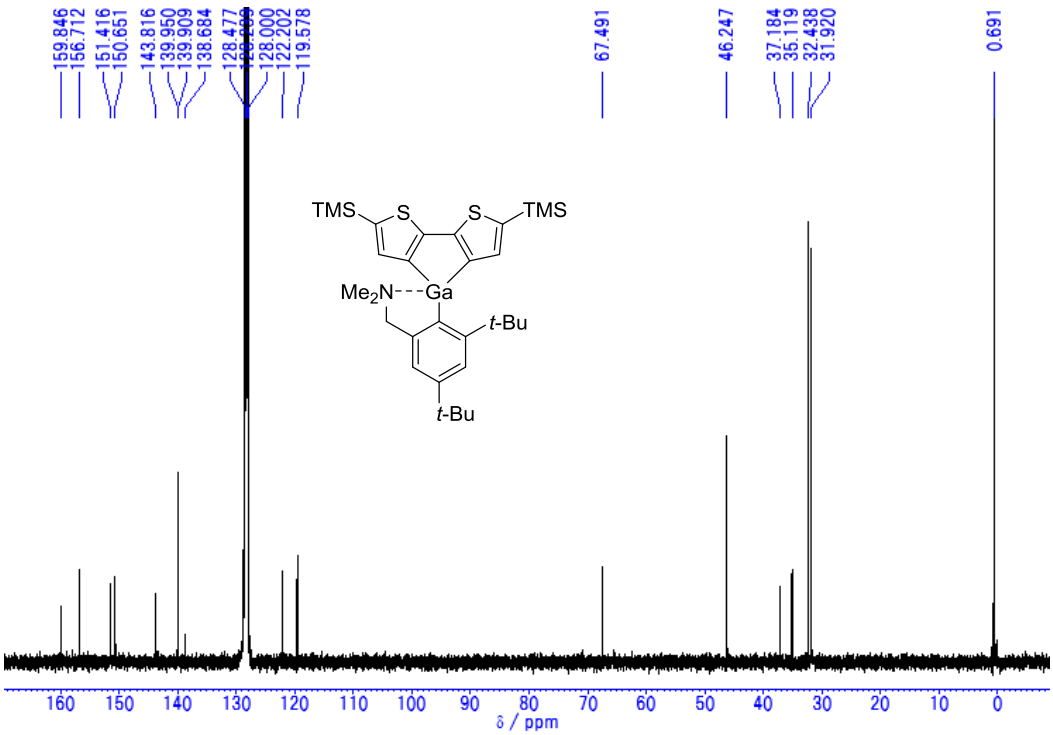

Figure S4. ^{13}C NMR spectrum of **GaDT-TMS** in C_6D_6.

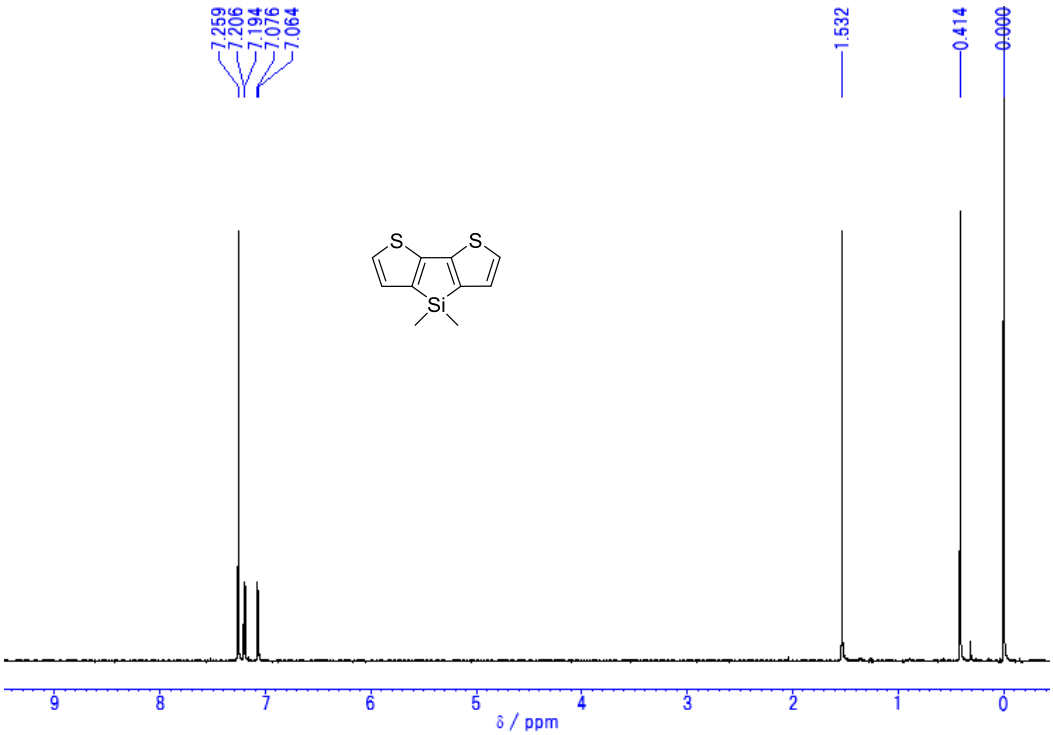

Figure S5. ^{1}H NMR spectrum of **SiDT** in $CDCl_3$.

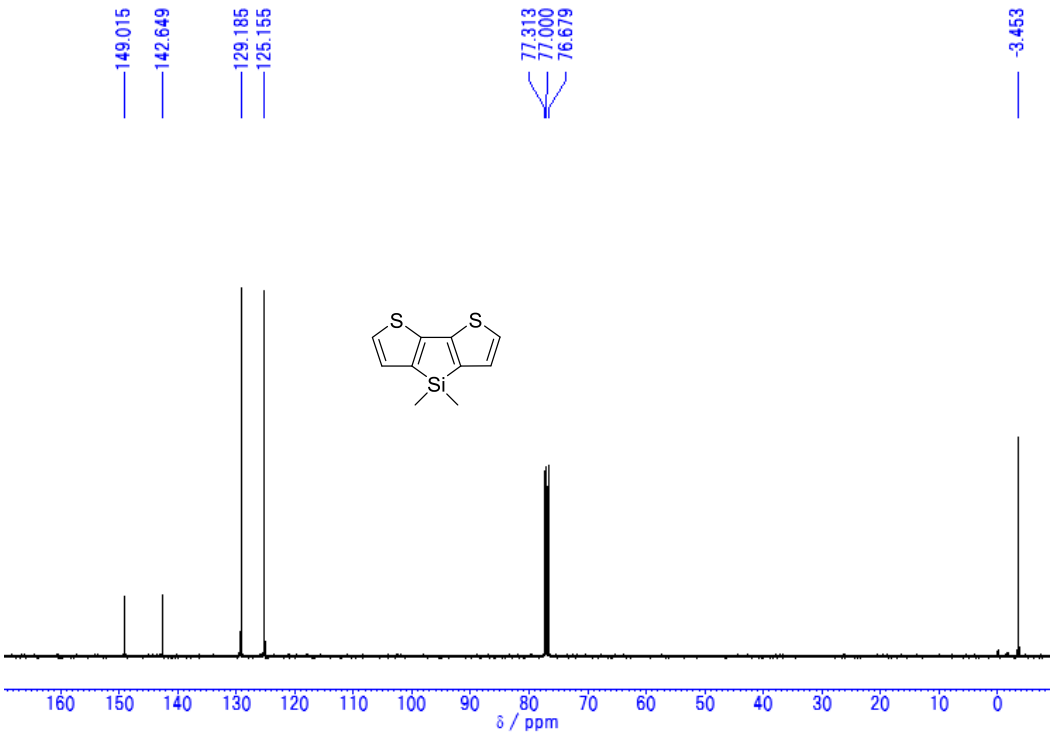

Figure S6. ^{13}C NMR spectrum of **SiDT** in $CDCl_3$.

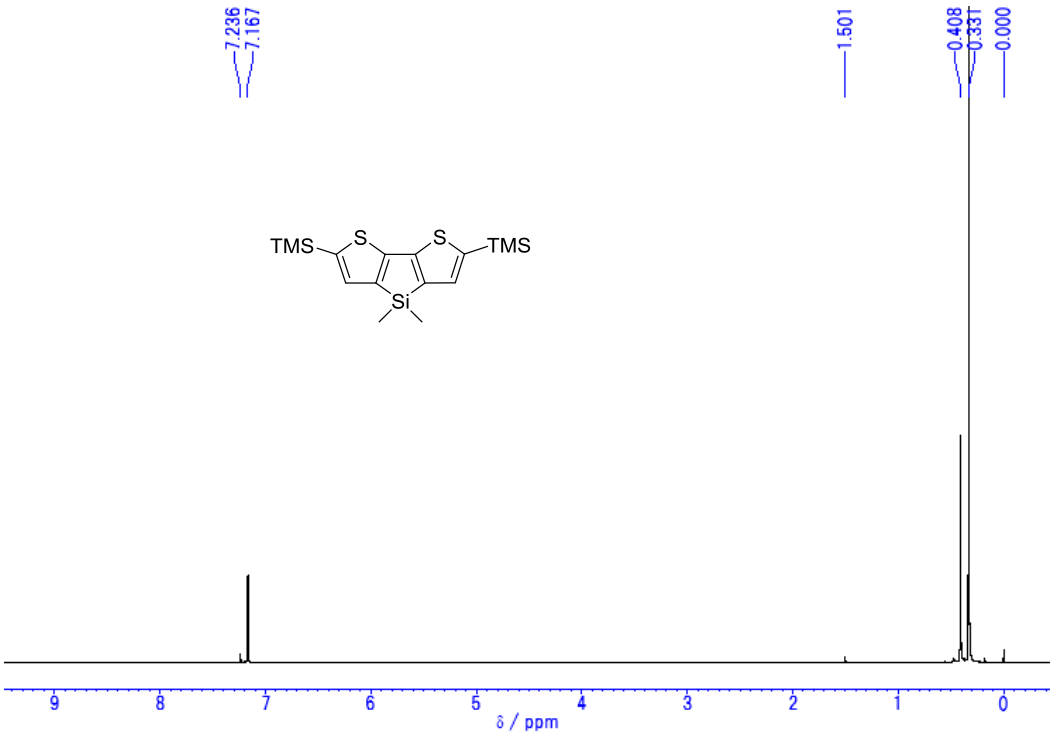

Figure S7. ^{1}H NMR spectrum of **SiDT-TMS** in $CDCl_3$.

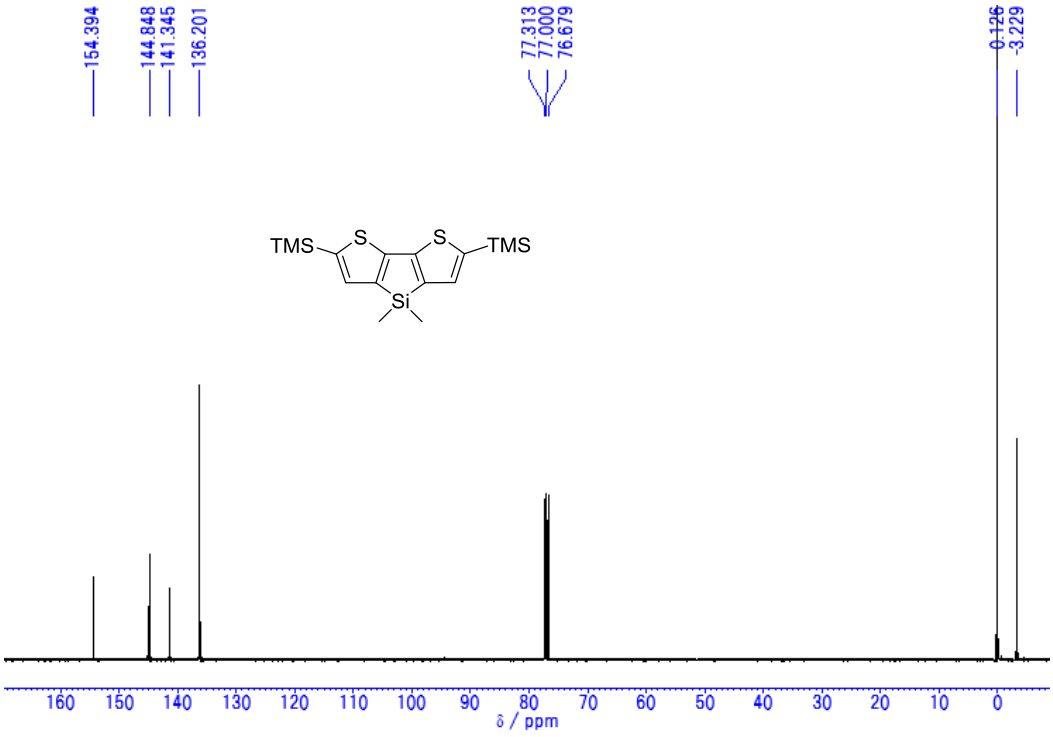

Figure S8. ^{13}C NMR spectrum of **SiDT-TMS** in $CDCl_3$.

X-ray Crystal Structure Analysis

Intensity data were collected on a Rigaku R-AXIS RAPID imaging plate area detector with graphite monochromated Mo *K*α radiation at –180 °C. The structures were solved by direct method (SIR97)[9] and refined by full-matrix least-squares procedures based on F^2 (SHELX-97).[10]

Table S1. Crystallographic data of **GaDT**

Empirical formula	$C_{25}H_{32}GaNS_2$
Formula weight	480.36
Temperature (K)	93(2)
Wavelength (Å)	0.71075
Crystal system, space group	monoclinic, *P21/c*
Unit cell dimensions	a = 8.0157(9)
	b = 25.291(3)
	c = 11.9431(15)
	α = 90.00
	β = 92.129(7)
	γ = 90.00
V (Å^3)	2419.5(5)
Z, calculated density (Mg m^{-3})	4, 1.319
Absorption coefficient	1.321
F(000)	1008
Crystal size (mm)	0.22 × 0.16 × 0.09
θ range for data collection	3.01–27.48
Limiting indices	$-10 \le h \le 10$, $-32 \le k \le 32$, $-15 \le l \le 15$
Reflections collected (unique)	21713/5527 [R(int) = 0.0545]
Completeness to theta = 27.48	0.993
Max. and min. transmission	0.8792 and 0.6927
Goodness-of-fit on F^2	1.033
Final R indices [$I > 2\sigma(I)$][a]	R_1 = 0.0458 wR_2 = 0.1032
R indices (all data)	R_1 = 0.0698, wR_2 = 0.1129

[a] $R_1 = \Sigma(|F_0|-|F_c|)/\Sigma|F_0|$. w$R_2 = [\Sigma w(F^2_0-F^2_c)^2/\ \Sigma w(F^2_0)^2]^{1/2}$. $w = 1/[\sigma^2(F^2_0)+[(ap)^2+bp]]$, where $p = [\max(F^2_0,0)+2F^2_c]/3$.

Table S2. Crystallographic data of **GaDT-TMS**

Empirical formula	$C_{32}H_{49}Cl_3GaNS_2Si$
Formula weight	744.09
Temperature (K)	93(2)
Wavelength (Å)	0.71075
Crystal system, space group	monoclinic, *P21/c*
Unit cell dimensions	a = 11.6396(7)
	b = 14.2359(9)
	c = 23.9678(16)
	α = 90.00
	β = 90.00
	γ = 90.00
V (Å^3)	3971.5(4)
Z, calculated density (Mg m^{-3})	4, 1.244
Absorption coefficient	1.081
F(000)	1560
Crystal size (mm)	0.21 × 0.16 × 0.12
θ range for data collection	3.09–27.47
Limiting indices	$-14 \le h \le 15$, $-18 \le k \le 18$, $-31 \le l \le 31$
Reflections collected (unique)	38324/9066 [R(int) = 0.1138]
Completeness to theta = 27.47	0.996
Max. and min. transmission	0.8812 and 0.8048
Goodness-of-fit on F^2	1.012
Final R indices [$I > 2\sigma(I)$][a]	R_1 = 0.0753 wR_2 = 0.1647
R indices (all data)	R_1 = 0.1402, wR_2 = 0.1911

[a] $R_1 = \Sigma(|F_0|-|F_c|)/\Sigma|F_0|$. w$R_2 = [\Sigma w(F^2_0-F^2_c)^2/ \Sigma w(F^2_0)^2]^{1/2}$. $w = 1/[\sigma^2(F^2_0)+[(ap)^2+bp]]$, where $p = [\max(F^2_0,0)+2F^2_c]/3$.

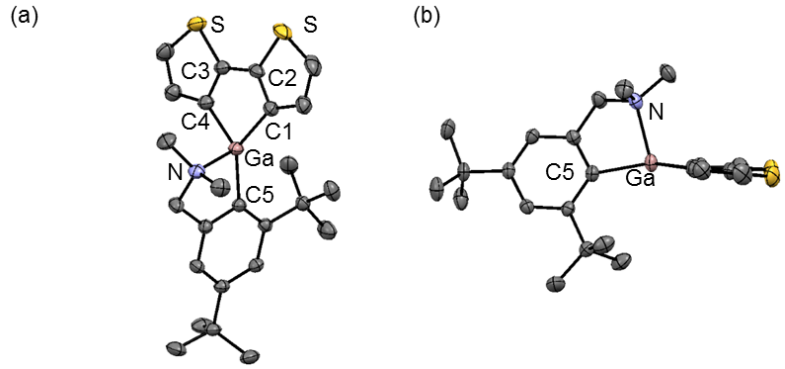

Figure S9. ORTEP drawings of (a) **GaDT** and (b) side view (30% probability for thermal ellipsoids). Hydrogen atoms are omitted for clarity.

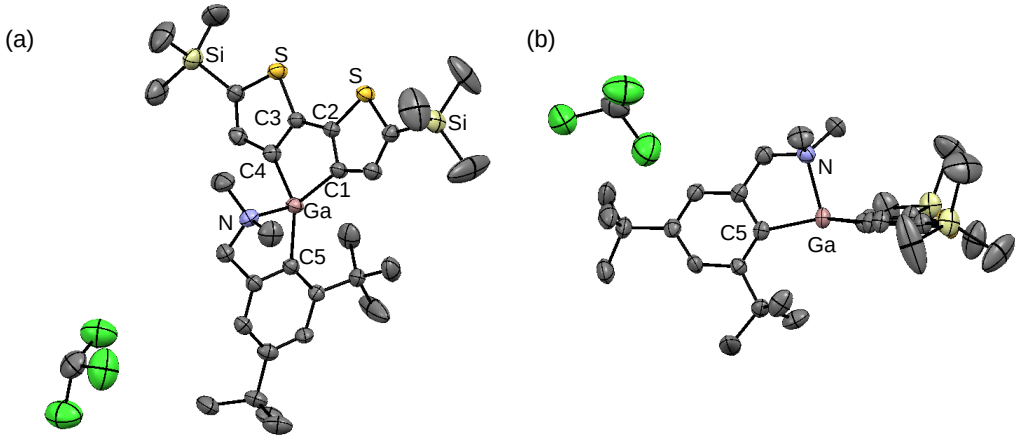

Figure S10. ORTEP drawings of (a) **GaDT-TMS**·$CHCl_3$ and (b) side view (30% probability for thermal ellipsoids). Hydrogen atoms are omitted for clarity.

Table S3. Selected bond lengths [Å] and angles [degree] for **GaDT** and **GaDT-TMS**

	GaDT	**GaDT-TMS**
Ga–N	2.091	2.090
Ga–C1	1.983	1.982
C1–C2	1.367	1.359
C2–C3	1.460	1.469
C3–C4	1.378	1.390
C4–Ga	2.004	2.012
Ga–C5	1.971	1.988
φC1–C2–C3–C4	3.7	1.7
Ga–C1–C2	105.7	106.8
C1–C2–C3	119.8	119.1
C2–C3–C4	119.4	119.8
C3–C4–Ga	104.9	104.5
C1–Ga–C4	89.9	89.79
C1–Ga–C5	138.9	133.93
C4–Ga–C5	125.6	130.85
Sum of C–Ga–C	354.5	354.6
C1–Ga–N	104.6	106.1
C4–Ga–N	105.7	103.0
C5–Ga–N	86.4	87.0
Sum of C–Ga–N	296.7	296.2

UV−vis absorption and photoluminescence (PL) data

Table S4. UV−vis absorption and PL data for dithienoheteroles[a]

	$\lambda_{max,abs}$ (nm)[b]	$\varepsilon_{max,abs}$ ($M^{-1}cm^{-1}$)[c]	$\lambda_{onset,abs}$ (nm)[d]	$\lambda_{max,FL}$ (nm)[e]	Φ_F[f]	$\tau_{1/2}$ (ns)[g]
GaDT	342	8.1×10^3	377	412	0.52	5.63 (100%) (χ^2 = 1.09)
GaDT-TMS	355	1.6×10^4	390	416	0.89	3.74 (100%) (χ^2 = 1.04)
SiDT	338	1.0×10^4	374	408	0.54	5.20 (100%) (χ^2 = 0.98)
SiDT-TMS	350	1.9×10^4	385	416	0.76	3.82 (100%) (χ^2 = 0.81)
CDT	316	1.9×10^4	344	373	0.05	< 0.05
BT	304	1.0×10^4	343	362	0.13	< 0.05
NDT	290	2.4×10^4	317	—[h]	—[h]	—[h]
SDT[i]	297	2.7×10^4	314	—[h]	—[h]	—[h]

[a]Optical measurements were performed for 1.0×10^{-5} M in THF solution. [b]Absorption maxima. [c]Molar absorption coefficient at $\lambda_{max,abs}$. [d]Onset wavelength of absorption bands. [e]Fluorescence maxima excited at $\lambda_{max,abs}$. [f]Absolute quantum yield. [g]Photoluminescence decay analyses were performed upon 375 nm (292 nm for **CDT** and **BT**) excitation by a UV diode laser. [h]Not detected. [i]Dithieno[3,2-*b*:2',3'-*d*]thiophene.

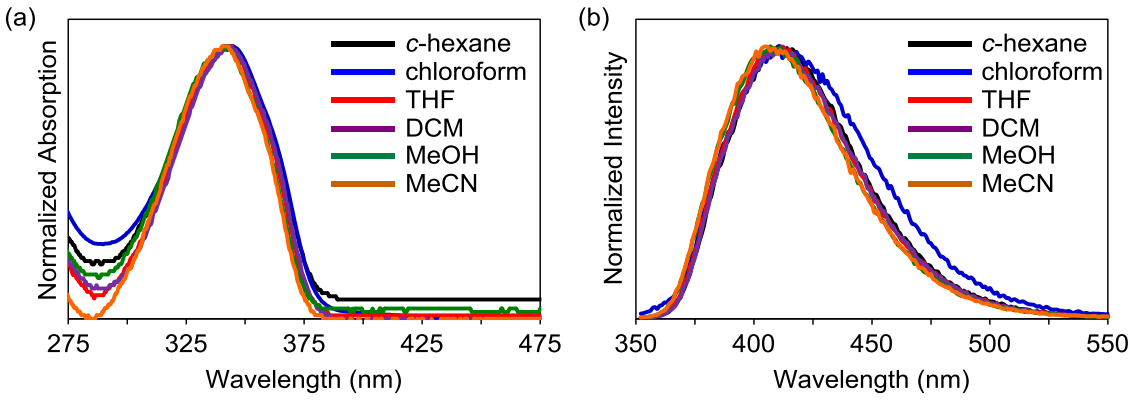

Figure S11. (a) UV−vis absorption and (b) PL (excited at $\lambda_{max, abs}$) spectra of 1.0×10^{-5} M **GaDT** in cyclohexane (black), chloroform (blue), THF (red), dichloromethane (purple), MeOH (green) and MeCN (orange).

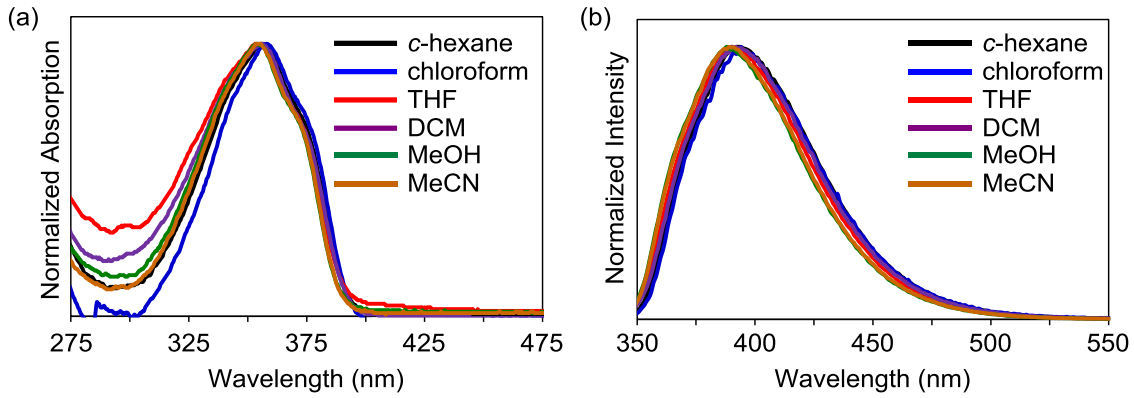

Figure S12. (a) UV−vis absorption and (b) PL (excited at $\lambda_{max,\ abs}$) spectra of 1.0×10^{-5} M **GaDT-TMS** in cyclohexane (black), chloroform (blue), THF (red), dichloromethane (purple), MeOH (green) and MeCN (orange).

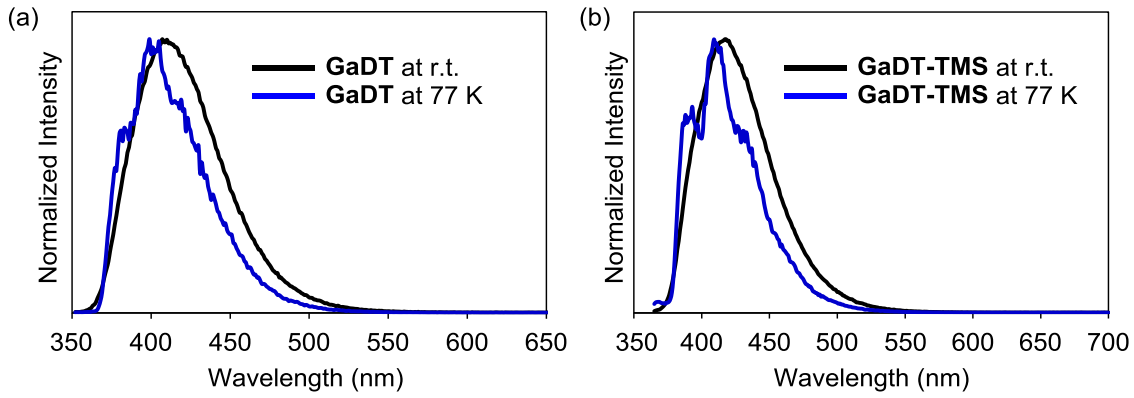

Figure S13. PL (excited at $\lambda_{max,\ abs}$) spectra of 1.0×10^{-5} M (a) **GaDT** and (b) **GaDT-TMS** in MeTHF at room temperature (black) and 77K (blue).

Density functional theory (DFT) calculation by Gaussian 09 program[12]

The optimized structure of **GaDT**, **GaDT-TMS**, **SiDT**, **SiDT-TMS**, **CDT**, **NDT'**, **SDT** and **BT** was obtained by DFT calculation at the B3LYP/6-31G(d,p) level. TD-DFT calculation was carried out at the B3LYP/6-311+G(2df) level for gallium atoms and the B3LYP/6-31G(d,p) level in order to estimate their electronic transitions.

Table S5. Cartesian coordinates of the optimized structure of **GaDT**

Center Symbol	Coordinates (Angstroms)		
	X	Y	Z
Ga	0.799791	−0.182576	−0.163261
S	4.541586	−0.802049	2.010670
S	4.876979	1.119599	−1.012902
C	−1.156322	0.001939	−0.032661
C	3.422201	0.421152	−0.346475
C	3.285576	−0.357669	0.881248
C	2.297667	0.703464	−1.109845
C	−5.526787	−0.432250	0.091167
C	−3.991719	−0.317502	0.037629
C	−1.982866	1.084601	0.338349
C	−3.165038	−1.376944	−0.337278
H	−3.587860	−2.338378	−0.610933
C	−1.777347	−1.211263	−0.367556
N	0.391515	−1.928600	−1.306982
C	2.033542	−0.810763	1.268143
C	−1.362146	2.460621	0.673157
C	−3.369371	0.898824	0.368364
H	−4.003842	1.728420	0.653623
C	−6.021896	−1.838870	−0.294492
H	−5.735841	−2.105905	−1.317250
H	−7.114660	−1.874163	−0.239100
H	−5.632482	−2.606989	0.381780
C	−6.017573	−0.128273	1.526631
H	−5.593122	−0.838689	2.243565
H	−7.109683	−0.202405	1.580669
H	−5.736516	0.878267	1.849489
C	2.110438	−1.518365	2.503171
H	1.253961	−1.957355	3.005615
C	−6.155847	0.584363	−0.890984
H	−5.872752	1.612870	−0.649339
H	−7.249442	0.522523	−0.856633
H	−5.836805	0.383427	−1.919055
C	−0.687197	3.023598	−0.599194
H	0.104727	2.353544	−0.940430
H	−0.235666	4.001614	−0.398173
H	−1.414048	3.140516	−1.410164
C	−0.885052	−2.396898	−0.698934

H	−0.622773	−2.933389	0.221212
H	−1.385768	−3.115379	−1.363586
C	1.463724	−2.938042	−1.219172
H	1.632596	−3.206999	−0.175699
H	2.392494	−2.505298	−1.597892
H	1.219071	−3.837001	−1.800481
C	2.638780	1.505397	−2.238002
H	1.918577	1.862401	−2.967463
C	3.376309	−1.606812	3.024002
H	3.702041	−2.083022	3.938725
C	3.972376	1.809204	−2.331553
H	4.483914	2.394742	−3.083096
C	−2.404786	3.485834	1.158322
H	−3.156218	3.703854	0.392377
H	−1.904800	4.429117	1.400469
H	−2.923433	3.146006	2.061082
C	0.181686	−1.528254	−2.716785
H	−0.087183	−2.396221	−3.333544
H	1.096739	−1.075014	−3.102297
H	−0.620424	−0.790049	−2.769783
C	−0.300162	2.310082	1.786060
H	−0.737200	1.880153	2.693149
H	0.131810	3.284199	2.038879
H	0.524278	1.660846	1.480080

Table S6. Cartesian coordinates of the optimized structure of **GaDT-TMS**

Center Symbol	Coordinates (Angstroms)		
	X	Y	Z
Ga	0.287981	−0.137963	−0.328510
S	−3.230127	2.390198	0.221759
S	−3.931702	−1.144927	0.092619
Si	−2.262130	5.425759	0.360535
Si	−4.200674	−4.322721	0.022337
C	5.074896	−0.410695	−0.124806
C	−1.341826	−1.254048	−0.198814
C	−2.387442	−0.351292	−0.045520
C	2.933360	−0.001932	−1.185635
C	−2.102958	1.078202	0.010055
C	2.222609	−0.336482	−0.018149
C	4.367274	−0.743213	1.038063
H	4.930260	−1.035793	1.912350
C	−0.790405	1.518521	−0.091827
C	2.135284	0.488648	−2.382492
H	1.978780	1.571570	−2.305072
H	2.658494	0.301471	−3.331169
C	4.324564	−0.039847	−1.246566
H	4.823551	0.221747	−2.176833
C	6.612907	−0.446679	−0.205627
C	2.965368	−0.720017	1.114718
N	0.787101	−0.143291	−2.397787
C	−5.519056	−4.312230	−1.336429
H	−5.065186	−4.229596	−2.329498
H	−6.207602	−3.468759	−1.217128
H	−6.114890	−5.231880	−1.314113
C	0.873837	−1.547085	−2.859394
H	−0.101987	−2.023711	−2.750368
H	1.595197	−2.089033	−2.245217
H	1.190066	−1.594320	−3.910077
C	−3.197458	−2.736600	−0.044894
C	−0.728769	2.934280	0.016278
H	0.202974	3.491177	−0.027892
C	2.243019	−1.138387	2.416653
C	−1.828641	−2.589346	−0.188210
H	−1.179086	−3.455238	−0.278309
C	1.281554	−0.017621	2.873969
H	0.508469	0.185938	2.128653
H	1.821792	0.918414	3.049378
H	0.772262	−0.301644	3.801133
C	−5.048606	−4.489369	1.706053
H	−5.722512	−3.647734	1.898634
H	−4.314101	−4.516031	2.517614
H	−5.642209	−5.409310	1.758820
C	7.142822	0.959959	−0.572418

H	6.751007	1.306157	−1.533486
H	8.236353	0.949171	−0.643423
H	6.859102	1.695258	0.187527
C	−3.013912	−5.772191	−0.243197
H	−3.557581	−6.722711	−0.205244
H	−2.238196	−5.804977	0.528920
H	−2.516586	−5.714545	−1.217008
C	−0.178689	0.605518	−3.223876
H	0.112130	0.606024	−4.282855
H	−0.256256	1.631389	−2.861599
H	−1.165840	0.149147	−3.120946
C	1.428358	−2.424012	2.142777
H	0.905055	−2.751357	3.048193
H	2.080118	−3.238424	1.808838
H	0.678467	−2.244138	1.369564
C	7.047956	−1.455708	−1.294914
H	6.655328	−1.186177	−2.279858
H	6.692581	−2.464027	−1.058408
H	8.140833	−1.489425	−1.370178
C	−1.940255	3.584107	0.183158
C	−0.602119	6.322398	0.213158
H	−0.131114	6.142280	−0.758794
H	0.099790	6.003551	0.990669
H	−0.741330	7.404229	0.317561
C	3.214044	−1.422936	3.578407
H	3.824717	−0.548336	3.826636
H	3.885863	−2.259216	3.359194
H	2.643102	−1.690580	4.473274
C	−3.045050	5.796326	2.043036
H	−3.240128	6.868698	2.158846
H	−2.389624	5.482958	2.862168
H	−3.998136	5.270305	2.163363
C	−3.430087	6.014180	−1.008612
H	−3.003073	5.830464	−2.000068
H	−3.628277	7.088671	−0.921795
H	−4.393385	5.494862	−0.962896
C	7.264399	−0.868696	1.124695
H	8.353859	−0.873225	1.016248
H	6.959703	−1.875450	1.428351
H	7.016797	−0.177325	1.936521

Table S7. Cartesian coordinates of the optimized structure of **SiDT**

Center Symbol	Coordinates (Angstroms)		
	X	Y	Z
S	−1.860843	−2.083189	0.000068
C	−0.727673	−0.765336	−0.000109
C	−3.198108	−0.964427	−0.000229
C	−2.775163	0.339435	−0.000092
C	−1.355395	0.473558	−0.000079
H	−4.210460	−1.344019	−0.000340
H	−3.469375	1.173097	−0.000105
C	0.727612	−0.765386	−0.000048
S	1.860695	−2.083314	0.000179
C	1.355416	0.473468	0.000045
C	2.775175	0.339250	0.000034
C	3.198036	−0.964640	−0.000296
Si	0.000058	1.791272	0.000048
H	3.469435	1.172872	0.000048
H	4.210365	−1.344293	−0.000506
C	−0.000051	2.865713	1.552171
C	0.000282	2.865733	−1.552068
H	−0.000465	2.249140	2.455711
H	0.884478	3.511274	1.583299
H	−0.884253	3.511755	1.582812
H	0.884922	3.511158	−1.583059
H	−0.000070	2.249150	−2.455602
H	−0.883812	3.511907	−1.582869

Table S8. Cartesian coordinates of the optimized structure of **SiDT-TMS**

Center Symbol	Coordinates (Angstroms)		
	X	Y	Z
S	1.863969	−1.373121	0.000029
C	0.726927	−0.063618	0.000041
C	3.233587	−0.266916	0.000015
C	2.770906	1.036888	0.000048
C	1.355047	1.176558	0.000019
Si	5.014809	−0.875567	−0.000010
H	3.455219	1.879789	0.000049
C	−0.726928	−0.063618	0.000029
S	−1.863970	−1.373120	−0.000039
C	−1.355048	1.176558	0.000007
C	−2.770907	1.036889	0.000020
C	−3.233588	−0.266915	0.000003
Si	0.000000	2.495511	−0.000009
H	−3.455220	1.879790	0.000033
Si	−5.014810	−0.875566	0.000003
C	0.000002	3.571463	−1.551494
C	0.000006	3.571501	1.551449
H	−0.000054	2.955447	−2.455450

H	−0.884381	4.217295	−1.581984
H	0.884440	4.217216	−1.582039
H	−0.884358	4.217360	1.581911
H	−0.000077	2.955507	2.455420
H	0.884464	4.217228	1.581988
C	−6.146654	0.638595	0.000082
C	−5.332896	−1.922237	−1.543759
C	−5.332846	−1.922368	1.543688
H	−4.670430	−2.793916	1.579925
H	−5.165476	−1.342275	2.457084
H	−6.365122	−2.290148	1.563189
H	−5.165553	−1.342067	−2.457111
H	−4.670483	−2.793784	−1.580091
H	−6.365175	−2.290013	−1.563260
H	−5.988893	1.262787	0.885776
H	−5.988918	1.262859	−0.885566
H	−7.196686	0.325726	0.000084
C	6.146653	0.638594	−0.000141
C	5.332930	−1.922204	1.543769
C	5.332809	−1.922404	−1.543678
H	4.670386	−2.793949	−1.579881
H	5.165422	−1.342330	−2.457083
H	6.365082	−2.290192	−1.563194
H	5.165604	−1.342015	2.457112
H	4.670523	−2.793753	1.580135
H	6.365211	−2.289973	1.563255
H	5.988875	1.262769	−0.885843
H	5.988935	1.262874	0.885499
H	7.196685	0.325723	−0.000157

Table S9. Cartesian coordinates of the optimized structure of **CDT**

Center Symbol	Coordinates (Angstroms)		
	X	Y	Z
S	2.021720	−1.831977	−0.000042
C	0.722110	−0.689352	0.000036
C	3.188200	−0.527751	0.000198
C	2.591989	0.708509	0.000055
C	1.174064	0.617535	−0.000005
H	4.243126	−0.763289	0.000304
H	3.158544	1.633126	0.000057
C	−0.722104	−0.689353	0.000020
S	−2.021715	−1.831983	−0.000144
C	−1.174065	0.617534	0.000006
C	−2.591988	0.708504	0.000093
C	−3.188197	−0.527759	0.000293
C	0.000000	1.597382	−0.000066
H	−3.158549	1.633117	0.000150
H	−4.243121	−0.763304	0.000481
C	−0.000013	2.480049	−1.267551
C	−0.000001	2.480138	1.267358
H	−0.000013	1.866724	−2.172466
H	−0.885385	3.124321	−1.288402
H	0.885349	3.124333	−1.288420
H	−0.885364	3.124417	1.288166
H	−0.000003	1.866882	2.172317
H	0.885368	3.124412	1.288172

Table S10. Cartesian coordinates of the optimized structure of **NDT'**

Center Symbol	Coordinates (Angstroms)		
	X	Y	Z
S	−2.086412	−1.644456	0.008585
C	−0.707771	−0.582110	0.002423
C	−3.173481	−0.265318	−0.003083
C	−2.527185	0.940746	−0.014624
C	−1.114180	0.759777	−0.015332
H	−4.239846	−0.441213	0.002280
H	−3.042713	1.893583	−0.018828
C	0.707601	−0.582239	0.002172
S	2.086113	−1.644729	0.008515
C	1.114214	0.759580	−0.015466
C	2.527227	0.940418	−0.014494
C	3.173380	−0.265730	−0.003004
N	0.000111	1.583450	−0.042571
H	3.042783	1.893239	−0.018662
H	4.239718	−0.441791	0.002285
C	0.000606	3.029214	0.044259
H	−0.887001	3.425178	−0.454833
H	0.008186	3.381849	1.083113
H	0.880417	3.425943	−0.468066

Table S11. Cartesian coordinates of the optimized structure of **BT**

Center Symbol	Coordinates (Angstroms)		
	X	Y	Z
S	−1.846146	1.191500	−0.224754
C	−0.715634	−0.119783	0.068633
C	−3.207380	0.129495	−0.051190
C	−2.814248	−1.155802	0.199693
C	−1.399139	−1.298955	0.269323
H	−4.210637	0.520456	−0.145894
H	−3.509426	−1.975353	0.340481
C	0.715633	0.119783	0.068654
H	−0.898869	−2.236964	0.482111
S	1.846149	−1.191511	−0.224671
C	1.399139	1.298941	0.269423
C	2.814246	1.155803	0.199718
C	3.207377	−0.129460	−0.051335
H	0.898872	2.236939	0.482262
H	3.509422	1.975358	0.340499
H	4.210631	−0.520396	−0.146175

Table S12. TD−DFT calculation result of **GaDT**

Transition Energy (Wave Length)	Assignment with Contribution	Oscillator Strength *f*
3.7106 eV (334.13 nm)	HOMO→LUMO (97.18%) HOMO→LUMO+9 (2.82%)	0.2538
3.988 eV (310.90 nm)	HOMO→LUMO+1 (100%)	0.0002
4.1624 eV (297.86 nm)	HOMO→LUMO+2 (100%)	0.0020
4.3639 eV (284.11 nm)	HOMO→LUMO+3 (42.57%) HOMO→LUMO+4 (57.43%)	0.0020
4.4066 eV (281.36 nm)	HOMO→LUMO+1 (2.69%) HOMO→LUMO+3 (31.41%) HOMO→LUMO+4 (28.05%) HOMO→LUMO+5 (23.21%) HOMO→LUMO+6 (8.57%) HOMO→LUMO+7 (6.07%)	0.0003
4.4274 eV (280.04 nm)	HOMO→LUMO+3 (25.07%) HOMO→LUMO+4 (14.06%) HOMO→LUMO+5 (49.91%) HOMO→LUMO+6 (4.33%) HOMO→LUMO+7 (6.63%)	0.0067
4.5057 eV (275.17 nm)	HOMO−6→LUMO (4.11%) HOMO−5→LUMO (4.36%) HOMO−1→LUMO (91.53%)	0.0046
4.5214 eV (274.21 nm)	HOMO→LUMO+5 (21.89%) HOMO→LUMO+6 (65.51%) HOMO→LUMO+7 (12.60%)	0.0025
4.5669 eV (271.49 nm)	HOMO→LUMO+5 (2.35%) HOMO→LUMO+6 (22.62%) HOMO→LUMO+7 (75.03%)	0.0001
4.7791 eV (259.43 nm)	HOMO−2→LUMO (85.49%) HOMO→LUMO+8 (2.68%) HOMO→LUMO+9 (11.83%)	0.0012

4.9205 eV (251.97 nm)	HOMO−3→LUMO (100%)	0.0002
4.9495 eV (250.50 nm)	HOMO−7→LUMO (2.97%) HOMO−6→LUMO (4.53%) HOMO−5→LUMO (2.71%) HOMO−4→LUMO (60.85%) HOMO→LUMO+8 (25.29%) HOMO→LUMO+9 (3.64%)	0.0740

Table S13. TD−DFT calculation result of **GaDT-TMS**

Transition Energy (Wave Length)	Assignment with Contribution	Oscillator Strength *f*
3.5684 eV (347.45 nm)	HOMO→LUMO (100%)	0.5131
3.9671 eV (312.53 nm)	HOMO→LUMO+1 (97.39%) HOMO→LUMO+5 (2.61%)	0.0001
4.1782 eV (296.74 nm)	HOMO→LUMO+2 (79.47%) HOMO→LUMO+3 (20.53%)	0.0028
4.2754 eV (290.00 nm)	HOMO→LUMO+2 (20.19%) HOMO→LUMO+3 (79.81%)	0.0040
4.3346 eV (286.03 nm)	HOMO−6→LUMO (8.56%) HOMO−1→LUMO (91.44%)	0.0048
4.3808 eV (283.02 nm)	HOMO→LUMO+4 (95.97%) HOMO→LUMO+5 (4.03%)	0.0094
4.4067 eV (281.35 nm)	HOMO→LUMO+1 (2.12%) HOMO→LUMO+4 (5.17%) HOMO→LUMO+5 (92.71%)	0.0126
4.5080 eV (275.03 nm)	HOMO→LUMO+5 (2.72%) HOMO→LUMO+6 (97.28%)	0.0045
4.5884 eV (270.21 nm)	HOMO−2→LUMO (57.61%) HOMO→LUMO+7 (39.87%) HOMO→LUMO+9 (2.52%)	0.0043
4.6263 eV (268.00 nm)	HOMO−2→LUMO (23.98%) HOMO→LUMO+7 (51.81%) HOMO→LUMO+9 (24.21%)	0.0004
4.7566 eV (260.66 nm)	HOMO−5→LUMO (12.27%) HOMO−4→LUMO (53.35%) HOMO→LUMO+8 (34.37%)	0.0374
4.7937 eV (258.64 nm)	HOMO−6→LUMO (3.69%) HOMO−3→LUMO (92.61%) HOMO−1→LUMO (3.70%)	0.0006

Table S14. TD−DFT calculation result of **SiDT**

Transition Energy (Wave Length)	Assignment with Contribution	Oscillator Strength *f*
3.8648 eV (320.80 nm)	HOMO→LUMO (97.87%) HOMO→LUMO+3 (2.13%)	0.3437
4.6341 eV (267.55 nm)	HOMO→LUMO+1 (100%)	0.0000
4.8878 eV (253.66 nm)	HOMO−1→LUMO (87.72%) HOMO→LUMO+3 (12.28%)	0.0019
4.9957 eV (248.18 nm)	HOMO−3→LUMO (9.09%) HOMO−2→LUMO (68.22%) HOMO→LUMO+2 (22.69%)	0.0708
5.3420 eV (232.09 nm)	HOMO−3→LUMO (38.33%) HOMO−2→LUMO (25.01%) HOMO−1→LUMO+2 (2.21%) HOMO→LUMO+2 (31.30%) HOMO→LUMO+8 (3.16%)	0.1095

Table S15. TD−DFT calculation result of **SiDT-TMS**

Transition Energy (Wave Length)	Assignment with Contribution	Oscillator Strength *f*
3.4664 eV (357.68 nm)	HOMO→LUMO (100%)	0.4652
4.6372 eV (267.37 nm)	HOMO−1→LUMO (90.59%) HOMO−1→LUMO+3 (9.41%)	0.0041
4.7023 eV (263.67 nm)	HOMO→LUMO+1 (100%)	0.0000
4.7551 eV (260.74 nm)	HOMO−3→LUMO (6.65%) HOMO−2→LUMO (73.61%) HOMO→LUMO+2 (19.74%)	0.0472
5.0558 eV (245.23 nm)	HOMO−3→LUMO (47.28%) HOMO−2→LUMO (22.43%) HOMO−1→LUMO+2 (30.30%)	0.0592
5.3398 eV (232.19 nm)	HOMO−1→LUMO (9.04%) HOMO→LUMO+3 (90.96%)	0.2977

Table S16. TD−DFT calculation result of **CDT**

Transition Energy (Wave Length)	Assignment with Contribution	Oscillator Strength *f*
4.2091 eV (294.56 nm)	HOMO→LUMO (100%)	0.4845
4.705 eV (263.52 nm)	HOMO→LUMO+1 (100%)	0.0000
5.142 eV (241.12 nm)	HOMO−3→LUMO (13.74%) HOMO−1→LUMO (44.47%) HOMO→LUMO+2 (41.78%)	0.0424
5.1801 eV (239.35 nm)	HOMO−2→LUMO (83.71%) HOMO→LUMO+4 (16.29%)	0.0071
5.3468 eV (231.88 nm)	HOMO−3→LUMO (15.45%) HOMO−2→LUMO+2 (2.18%) HOMO−1→LUMO (48.32%) HOMO−1→LUMO+2 (30.30%) HOMO→LUMO+7 (3.76%)	0.0968

Table S17. TD−DFT calculation result of **NDT'**

Transition Energy (Wave Length)	Assignment with Contribution	Oscillator Strength *f*
4.3607 eV (284.32 nm)	HOMO→LUMO (100%)	0.4048
4.4647 eV (277.70 nm)	HOMO−1→LUMO (97.69%) HOMO→LUMO+7 (2.31%)	0.1064
4.7123 eV (263.11 nm)	HOMO−3→LUMO+1 (100%)	0.0008
5.0980 eV (243.20 nm)	HOMO−1→LUMO+1 (100%)	0.0000

Table S18. TD−DFT calculation result of **BT**

Transition Energy (Wave Length)	Assignment with Contribution	Oscillator Strength *f*
4.3601 eV (284.36 nm)	HOMO→LUMO (100%)	0.5823
5.0622 eV (244.92 nm)	HOMO−3→LUMO (11.14%) HOMO−1→LUMO (55.67%) HOMO→LUMO+1 (33.19%)	0.0017
5.1308 eV (241.65 nm)	HOMO−3→LUMO (2.74%) HOMO−1→LUMO (15.54%) HOMO→LUMO+1 (19.18%) HOMO→LUMO+2 (62.54%)	0.0008
5.2673 eV (235.38 nm)	HOMO−2→LUMO (59.41%) HOMO→LUMO+3 (37.03%) HOMO→LUMO+4 (3.56%)	0.0602

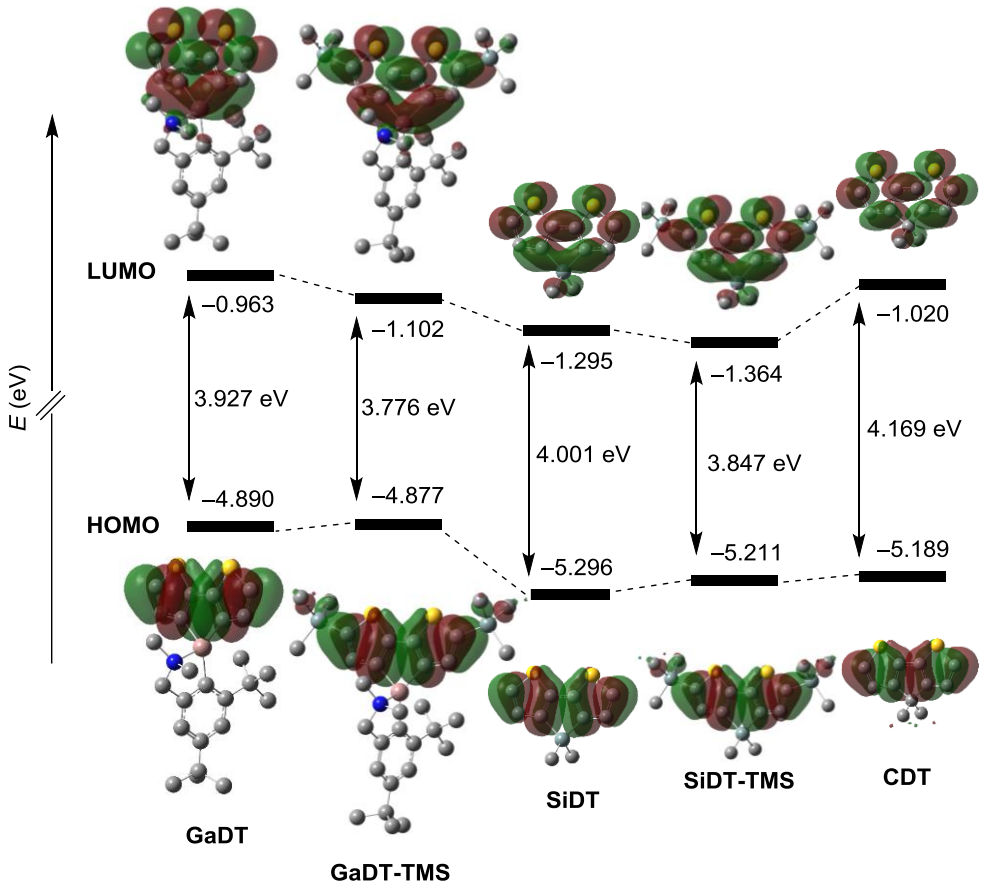

Figure S14. Energy diagram and frontier orbitals of **GaDT**, **GaDT-TMS**, **SiDT**, **SiDT-TMS** and **CDT** calculated by the DFT method. Hydrogen atoms are omitted for clarity.

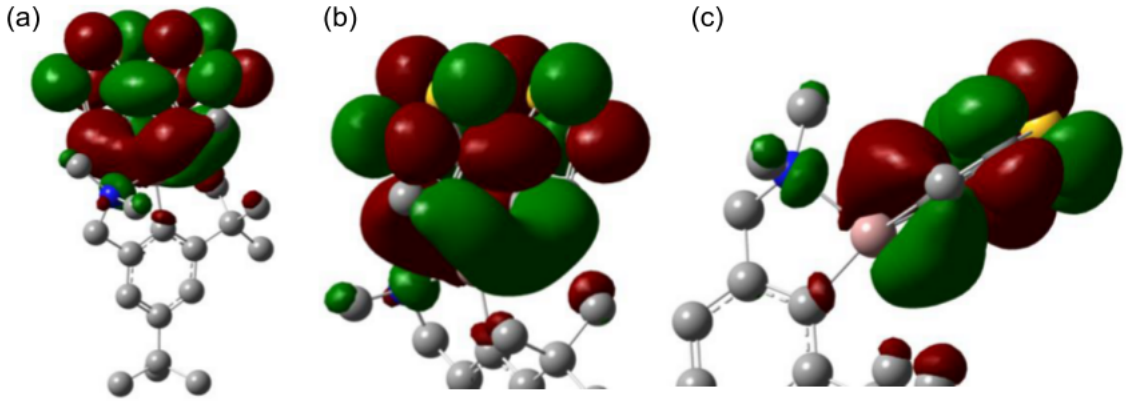

Figure S15. LUMO of **GaDT** (a: overall view, b: back view, c: side view) calculated by the DFT method. Hydrogen atoms are omitted for clarity.

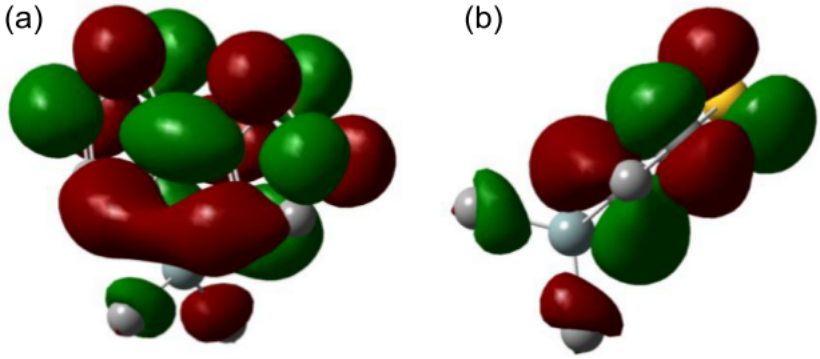

Figure S16. LUMO of **SiDT** (a: overall view, b: side view) calculated by the DFT method. Hydrogen atoms are omitted for clarity.

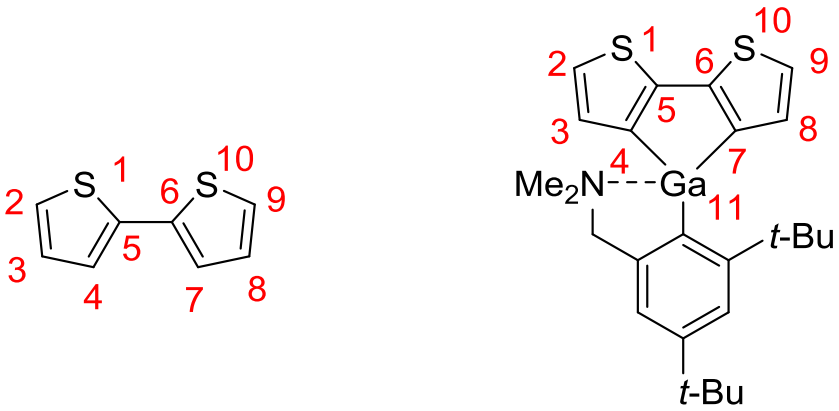

Figure S17. Labeled number of selected carbon and gallium atoms of **BT** and **GaDT**.

Table S19. NPA charges[a] of carbon and gallium atoms of **BT** and **GaDT**.

Number	Center Symbol	Natural Charge	
		BT	GaDT
1	S	0.45509	0.44436
2	C	−0.44014	−0.44853
3	C	−0.27738	−0.27445
4	C	−0.26360	−0.54026
5	C	−0.24007	−0.24952
6	C	−0.24007	−0.24423
7	C	−0.26360	−0.55009
8	C	−0.27739	−0.27636
9	C	−0.44014	−0.44882
10	S	0.45509	0.44863
11	Ga	–	1.49844

[a] Calculated at B3LYP/6-31G(d,p) levels.

References

(1) Higashi, T. *ABSCOR. Program for Absorption Correction.*; Rigaku Corporation: Japan, 1995.

(2) Sheldrick, G. M. SHELX-97. Programs for Crystal Structure Analysis.; University of Göttingen: Germany, **1997**.

(3) Altomare, A.; Burla, M. C.; Camalli, M.; Cascarano, G. L.; Giacovazzo, C.; Guagliardi, A.; Moliterni, A. G. G.; Polidori, G.; Spagna, R. *J. Appl. Cryst.* **1999,** *32*, 115–119.

(4) Wakita, K. *Yadokari-XG. Program for Crystal Structure Analysis.*; **2000**.

(5) (a) Yoshifuji, M.; Kamijo, K.; Toyota, K. *Tetrahedron Lett.* **1994**, *35*, 3971–3974. (b) Bagh, B.; Gilroy, J. B.; Staubitz, A.; Müller, J. *J. Am. Chem. Soc.* **2010**, *132*, 1794–1795.

(6) Hanamura, H.; Haneishi, R.; Nemoto, N. *Tetrahedron Lett.* **2011**, *52*, 4039–4041.

(7) Gaussian 09, Revision A.1, Frisch, M. J.; Trucks, G. W.; Schlegel, H. B.; Scuseria, G. E.; Robb, M. A.; Cheeseman, J. R.; Scalmani, G.; Barone, V.; Mennucci, B.; Petersson, G. A.; Nakatsuji, H.; Caricato, M.; Li, X.; Hratchian, H. P.; Izmaylov, A. F.; Bloino, J.; Zheng, G.; Sonnenberg, J. L.; Hada, M.; Ehara, M.; Toyota, K.; Fukuda, R.; Hasegawa, J.; Ishida, M.; Nakajima, T.; Honda, Y.; Kitao, O.; Nakai, H.; Vreven, T.; Montgomery, Jr., J. A.; Peralta, J. E.; Ogliaro, F.; Bearpark, M.; Heyd, J. J.; Brothers, E.; Kudin, K. N.; Staroverov, V. N.; Kobayashi, R.; Normand, J.; Raghavachari, K.; Rendell, A.; Burant, J. C.; Iyengar, S. S.; Tomasi, J.; Cossi, M.; Rega, N.; Millam, J. M.; Klene, M.; Knox, J. E.; Cross, J. B.; Bakken, V.; Adamo, C.; Jaramillo, J.; Gomperts, R.; Stratmann, R. E.; Yazyev, O.; Austin, A. J.; Cammi, R.; Pomelli, C.; Ochterski, J. W.; Martin, R. L.; Morokuma, K.; Zakrzewski, V. G.; Voth, G. A.; Salvador, P.; Dannenberg, J. J.; Dapprich, S.; Daniels, A. D.; Farkas, Ö.; Foresman, J. B.; Ortiz, J. V.; Cioslowski, J.; Fox, D. J. Gaussian, Inc., Wallingford CT, **2009**.